

RESEARCH

Open Access



Synthesis of nanosize zinc oxide through aqueous sol–gel route in polyol medium

Samreen Zahra^{1*}, Hamim Bukhari², Saboora Qaisar², Asma Sheikh³ and Athar Amin¹

Abstract

Background: This study is aimed to synthesize nanosize zinc oxide by acid catalyzed sol–gel process using zinc nitrate hexahydrate as precursor, aqueous isopropanol as solvent and glycerin for making polyol system. The polyol mediated procedure was employed in combination with calcination induced synthesis of nanoparticles of numerous sizes obtained with the variation in calcination temperature from 500 to 900 °C. The crystal structure of the prepared samples was characterized by X-ray diffraction analysis (XRD). Infrared spectroscopy (IR) was used to identify the surface hydroxyl groups. Thermal stability was confirmed by differential scanning calorimetry-thermogravimetric analysis (DSC-TGA) whereas field emission scanning electron microscopy (FESEM) was used to study the surface morphology of nanoparticles.

Results: Results revealed the formation of hexagonal wurtzite structure of irregular shaped nanoparticles having size ranging from 50–100 nm. However, the particles combined to form agglomerates of 200–400 nm with the rise in calcination temperature.

Conclusions: These results indicate that nanosize zinc oxide can be synthesized successfully by a simple process comprising of glycerin as a low-cost, non-toxic and eco-friendly polyol followed by calcination at ambient temperatures.

Keywords: Zinc oxide, Sol–gel process, Polyol system, Nanoparticles, Crystal structure, Surface morphology

Introduction

Zinc oxide (ZnO) has been found to be of great importance since it exhibits such semiconducting, pyroelectric, piezoelectric, optoelectronic and catalytic properties that make it a multi-functional material for use in biosensors, light emitting diodes, field effect transistors, ferromagnetic materials for spintronics solar cells, photocatalysis, antibacterial and antioxidants. It possesses a wide band gap of 3.37 eV with high binding energy i.e. 60 meV.

Nanoscale ZnO possesses improved properties as compared to its bulk counterpart and therefore can be used in numerous products including rubber, electrophotography, photoprinting, capacitors, protective coatings, anti-microbial, and conductive thin-films in LCDs, blue laser diodes medicines, cosmetics and food items [1–3]. Gunalan et al. found zinc oxide nanoparticles quite active against various bacterial and fungal pathogens and proposed that these nanoparticles can be efficiently employed in agriculture and food safety [4].

As reported previously, a variety of conventional methods have been employed for the synthesis of zinc oxide nanoparticles like sol–gel method, anodization, co-precipitation, ultrasound, chemical vapor deposition (CVD) and mechanochemical-thermal synthesis [5]. Yahya and

*Correspondence: samreenzahra68@hotmail.com

¹ Mineral Processing Research Centre, PCSIR Laboratories Complex, Ferozpur Road, Lahore 54600, Pakistan

Full list of author information is available at the end of the article



co-workers prepared zinc oxide nanoparticles by precipitation and self-combustion method for their potential use as a solar cell [6]. However, synthesis of zinc oxide by sol-gel method has been found to be simple and capable of producing particles with smaller size having larger specific surface area and high purity as compared to the other methods. Sol-gel synthesis of ZnO has been reported by many of the previous scientists [2, 7–9]. Recently, Vishwakarma et al. obtained ultra-fine zinc oxide particles of average particle size 58.3 nm via sol-gel process [10]. More recently, Somoghi et al. synthesized zinc oxide coatings modified with different silane coupling agents i.e. octyltriethoxysilane, octadecyltriethoxysilane and 3-glycidyloxypropyl trimethoxysilane using sol-gel method and concluded that these coatings can be highly suitable for industrial applications [11]. During the last decade, some researchers have adopted procedures mediated by polyalcohols (diethylene glycol, triethylene glycol, polyvinyl alcohol) for the synthesis of zinc oxide nanorods, nanoclips and nanospheres [12–17].

The current study has therefore been carried out to synthesize zinc oxide particles through polyol mediated sol-gel method followed by calcination induced process at various temperatures i.e. 500 °C, 700 °C and 900 °C. The phase composition, purity, thermal stability and surface morphology of the prepared samples were studied using X-ray diffraction technique, infrared spectroscopy, differential thermal analysis and field emission scanning electron microscopy.

Experimental

Reagents

Zinc nitrate hexahydrate (Sigma-Aldrich; 99%), isopropyl alcohol (WINLAB; 99%), glycerin (BDH; 99%) and nitric acid (Merck; 65%).

Synthesis of zinc oxide nanoparticles

Zinc oxide nanoparticles were synthesized through aqueous sol-gel route in acidic medium. 14.64 g of zinc nitrate hexahydrate were added to a mixture of solvents i.e. isopropyl alcohol and water in 1:4 ratio. 10 mL of glycerin were added and pH of the aqueous solution was maintained at 1 using nitric acid. The mixture was stirred constantly for two hours at 70 °C. The sol formed was also dried at 70 °C for 24 h. The gel thus obtained was ground and was divided into three portions that were calcined for two hours at 500 °C, 700 °C and 900 °C and were labeled as ZNA-1, ZNA-2 and ZNA-3 respectively. The graphical representation of the process is shown in Fig. 1.

Characterization

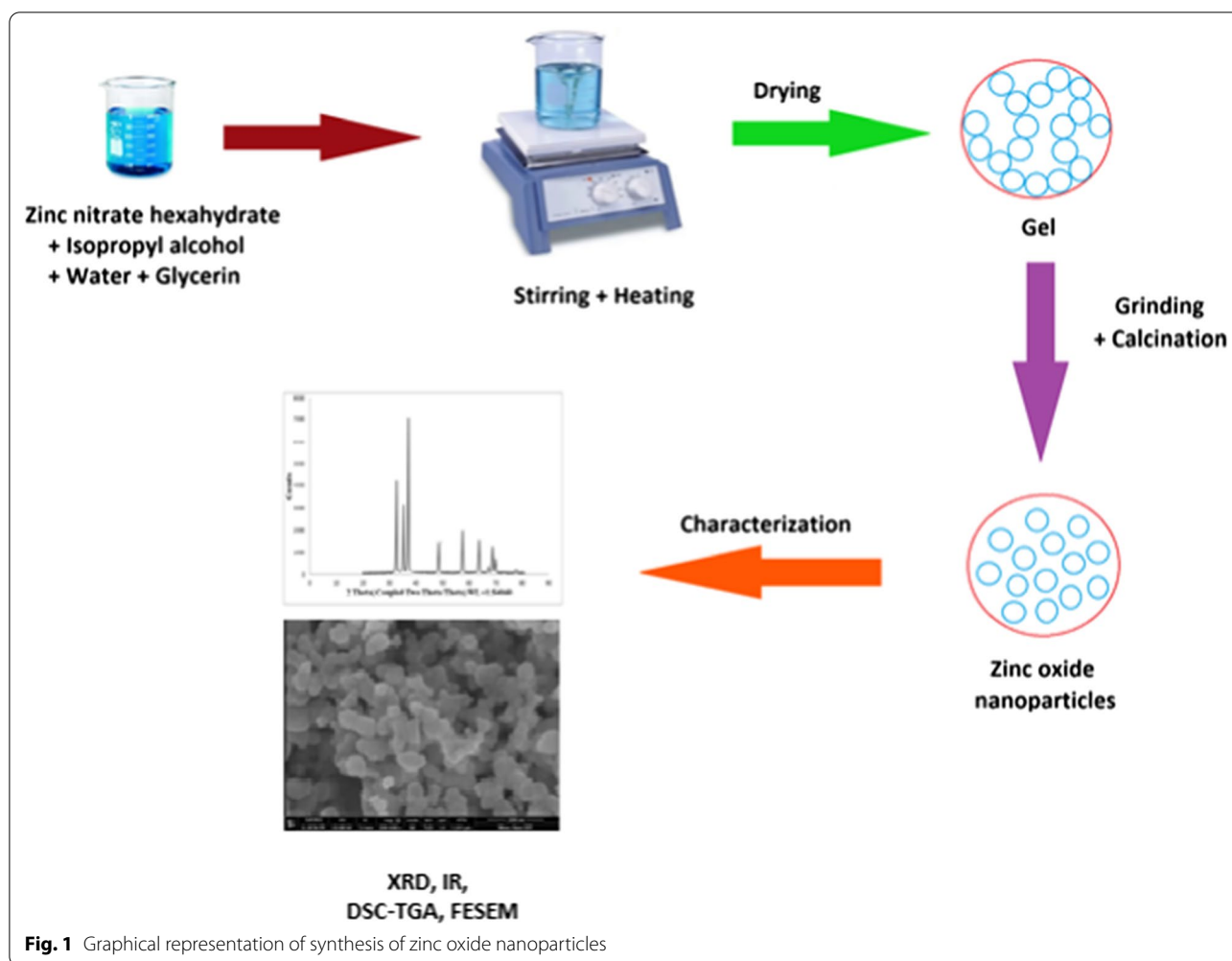
The crystal structure of all the prepared zinc oxide samples was identified by Bruker D2-Phaser X-ray diffractometer by monochromatized $\text{CuK}\alpha_1$ radiation at a wavelength of 1.54060 Å. IR spectroscopy was performed with Thermo Nicolet IR 200 (USA). DSC-TGA was carried out using differential scanning calorimeter Universal V4.5A, TA instruments USA. Surface morphology was studied using field emission scanning electron microscope FEI Nova 450 NanoSEM.

Results and discussion

Zinc oxide nanoparticles were prepared via polyol mediated solgel process and were calcined at 500 °C, 700 °C and 900 °C. The synthesis was carried out in acidic medium using aqueous isopropanol as solvent and glycerin as a polyol. A previous investigation revealed that surface morphology and other physical characteristics of metal oxide nanoparticles are highly dependent on the nature of solvents used. Solvent like isopropanol plays a vital role in enhancing the physical properties of nanoparticles thereby improving their catalytic properties manifolds as compared to their bulk counterparts [18]. Another observation about metal oxide nanoparticles obtained through aqueous systems is that they are commonly formed as hard agglomerates that results in reduction of their surface area and hence affects their performance in various applications. The polyol medium, on the other hand, has proved to be a suitable alternative for inhibiting agglomeration since the polyol acts as both solvent as well as stabilizing agent. Moreover, use of high boiling polyol has been found to be more appropriate [19]. In this study, glycerin was therefore employed for controlling the nucleation and growth of zinc oxide nanoparticles. The prepared samples were characterized and results obtained are as follows:

X-ray diffraction analysis

X-ray diffraction analysis of the synthesized ZNA samples was conducted to identify their crystalline structure and phase purity and diffractograms are illustrated in Figs. 2a, b and c. As observed in figures, the diffraction patterns for ZNA-1, ZNA-2 and ZNA-3 calcined at 500 °C, 700 °C and 900 °C respectively show various peaks corresponding to the hexagonal wurtzite phase of zinc oxide. The major peaks appear at 2θ values 31.93° and 36.33° corresponding to (100) and (101) planes while the other peaks confirming the presence of wurtzite structure can be seen at 2θ values 34.56°, 47.61°, 56.56°, 62.73°, 67.79° and 69.95° consistent with (002), (102), (110), (103), (200) and (201) planes



(JCPDS Card no: 36–1451). These results are in close agreement with the observations of previous scientists [1, 2, 15, 20–23].

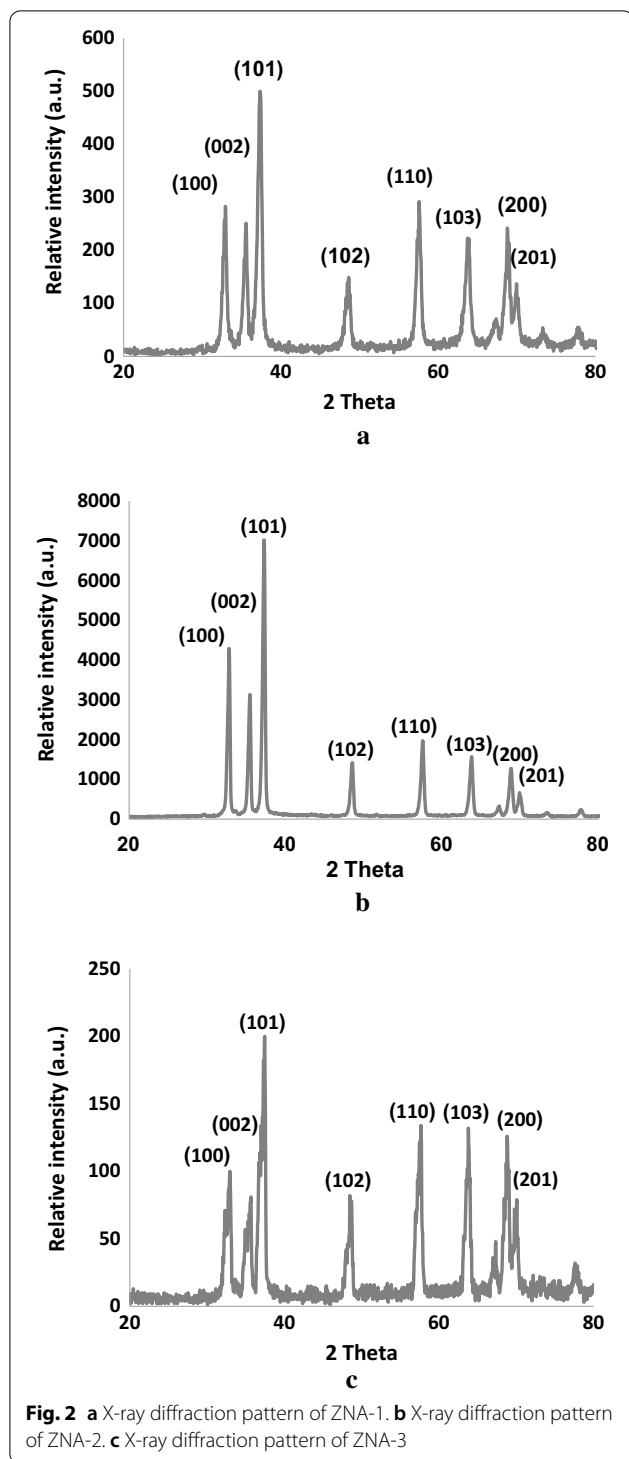
No other peaks are observed in the patterns which indicate the absence of impurities. Hence, XRD results reveal that similar diffraction peaks appear in case of all the three ZNA samples with no significant variation in intensities except ZNA-2 in which the major diffraction peaks appear to be relatively sharp as compared to ZNA-1 and ZNA-3. This observation can be attributed to lattice variation with the rising calcination temperature owing to the presence of dangling bonds on the surface of zinc oxide nanoparticles. Kayani et al. observed a decrease from 300 to 500 °C followed by an increase in lattice constants with further rise in calcination temperature [24].

Infrared spectroscopy

The IR spectra of ZNA samples recorded in the frequency range of 4000–400 cm^{-1} are demonstrated in

Figs. 3a, b and c. The spectra depict similar absorption bands with slight variation in intensities among all the samples. In the region between 3800 and 3000 cm^{-1} several absorption bands combined to form a broad band can be seen. This region corresponds to the combination of various stretching vibrations of hydroxyl groups of surface adsorbed water molecules and hydrogen bonded hydroxyl groups [25, 26]. However, it can be seen that absorption bands become relatively distinct with the rise in calcination temperature probably due to particle growth.

The bands of minor intensities between 3000 and 2800 cm^{-1} can be ascribed to the stretching vibrations of alkyl groups of organic impurities entangled in the nanocrystals during their synthesis [27]. Many less intense absorption bands in the region 2800–2200 cm^{-1} appear due to strong hydrogen bonding between water molecules. The absorption bands around 1600 cm^{-1} are attributed to the bending vibrational modes of hydroxyl groups of water molecules [28–30]. Another



minor absorption band at 1384.72 cm^{-1} associated with asymmetric stretching vibrations of nitrate group can be observed in case of ZNA-1, however, no such bands appeared for ZNA-2 and ZNA-3 [31].

The prominent broad band below 1000 cm^{-1} with high intensity in case of ZNA-2 and ZNA-3 and relatively less intensity for ZNA-1, signifies the presence of Zn–O bonds of zinc oxide since metal oxides generally exhibit absorption bands in fingerprint region below 1000 cm^{-1} [32]. Recently, Jayachandran et al. obtained multiple sharp bands at 491 cm^{-1} and 435 cm^{-1} attributed to the presence of Zn–O bonds [33]. Mahamuni and co-workers also observed bands corresponding to the stretching vibrations of Zn–O around $415\text{--}480\text{ cm}^{-1}$. According to them slight variations in wavenumbers and frequencies are consistent with the variety of particle sizes of metal oxides [15].

Thermal analysis

Thermal behavior of the prepared zinc oxide samples ZNA-1, ZNA-2 and ZNA-3 was investigated by DSC-TGA and curves are shown in Figs. 4a, b and c respectively. The TGA curve presented in Fig. 4a offers a two-step loss below $700\text{ }^{\circ}\text{C}$ in case of ZNA-1. In the initial step, an abrupt weight loss of 1.26% with a corresponding endothermic peak shown in DSC curve till $200\text{ }^{\circ}\text{C}$ is ascribed to the evaporation of adsorbed moisture [34]. In another step in the temperature range of $200\text{--}690\text{ }^{\circ}\text{C}$, a gradual weight loss of 0.31% resulted due to the removal of organic residues entrapped between the crystals during their synthesis [15]. In addition, a negligible weight gain of 0.03% noticed from 690 to $1000\text{ }^{\circ}\text{C}$ can be attributed to the heat transfer between sample and crucible. Both these stages are accompanied with an endothermic peak that continues from 200 to $1000\text{ }^{\circ}\text{C}$ with a gradual but continuous change in heat absorbed by the sample.

Figure 4b illustrates a net weight loss of 0.78% for ZNA-2 with four stages of trivial changes in weight i.e. three stages of weight loss analogous to ZNA-1 while an additional stage comprising of a weight gain of 0.14% from 550 to $870\text{ }^{\circ}\text{C}$ due to organic residues entrapped by the mesopores present between the crystallites. However, the resulting DSC curve appears to be similar to that of ZNA-1. ZNA-3 (Fig. 4c) also showed a weight loss of 0.82% ascribed to physically adsorbed moisture and organic residues with a corresponding endothermic peak exhibited in DSC curve like ZNA-1. Among previous scientists Khan et al. observed 48.14, 48.30, 51.34 and 55.55% residues among various zinc oxide samples indicating 51.86, 51.70, 48.66 and 44.45% weight loss respectively at $450\text{ }^{\circ}\text{C}$ [8]. However, thermal changes observed among the synthesized ZNA samples indicate complete transformation of the precursor to zinc oxide and hence, confirm their purity.

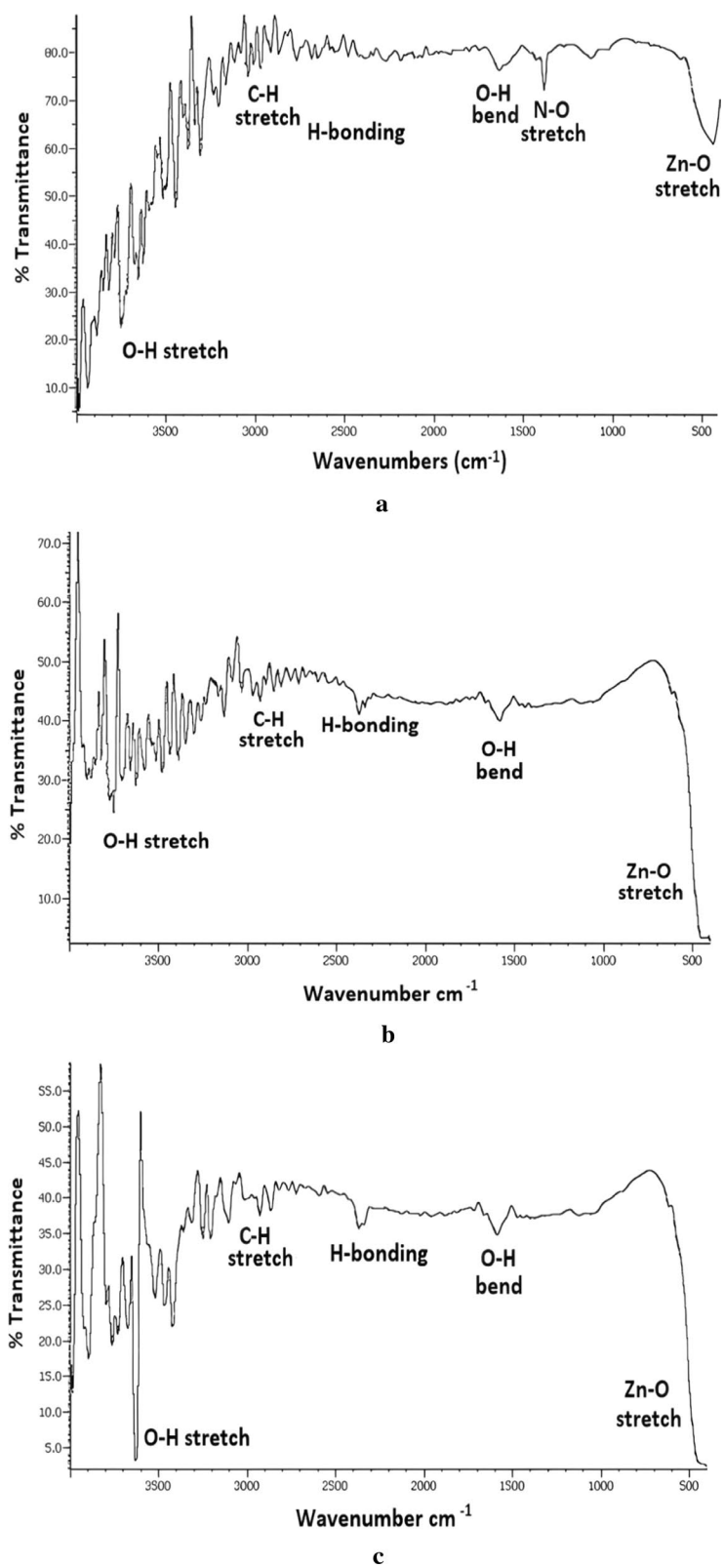
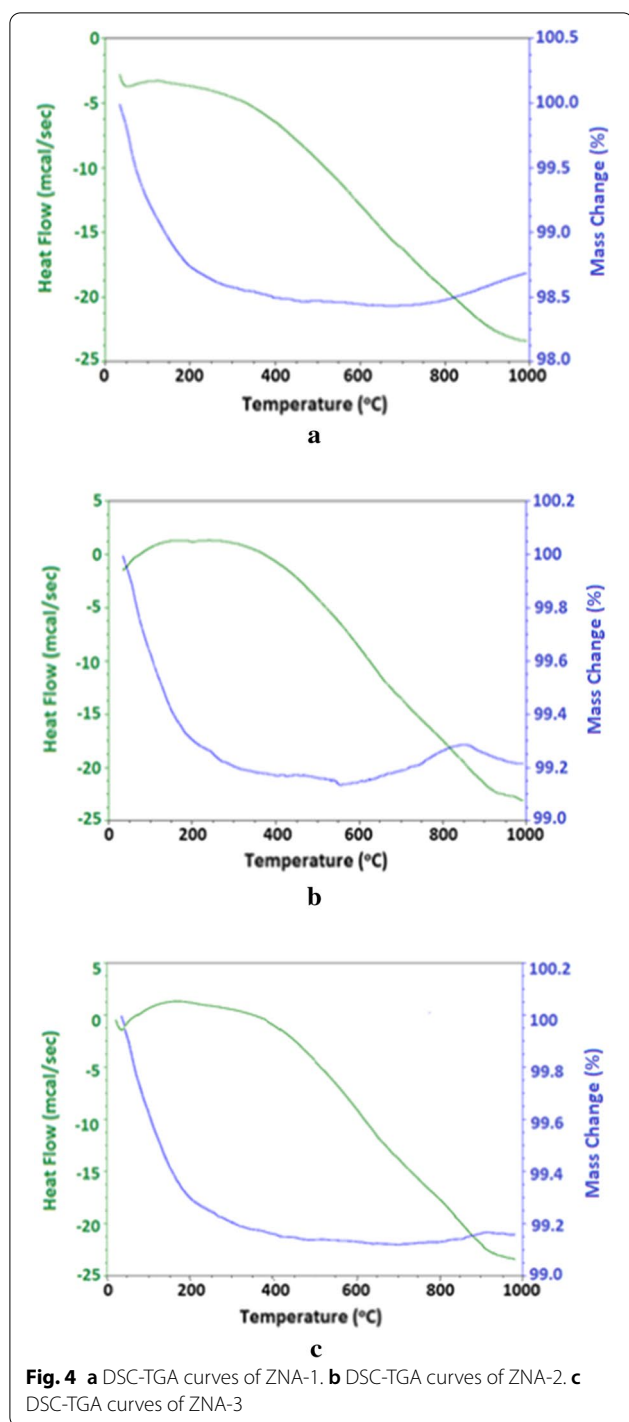
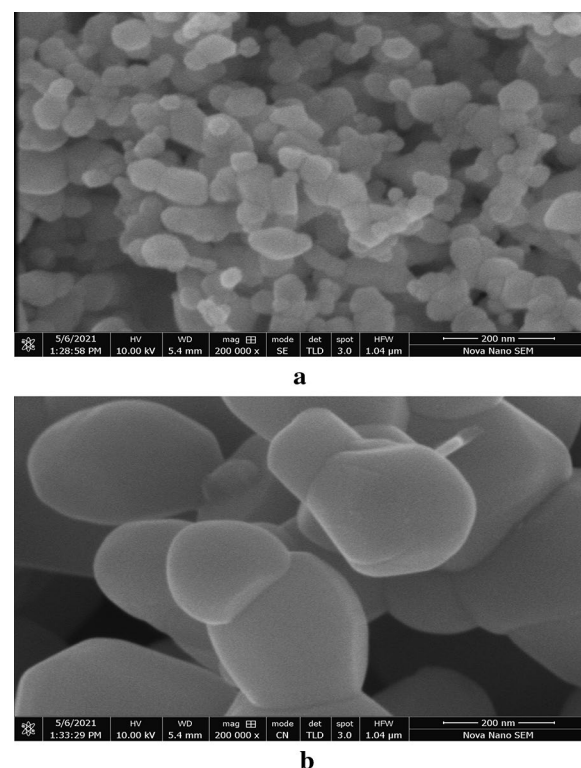


Fig. 3 a IR spectrum of ZNA-1. b IR spectrum of ZNA-2. c IR spectrum of ZNA-3



Field emission scanning electron microscopy

Surface morphology of ZNA-1 and ZNA-3 was studied by field emission scanning electron microscopy. The images recorded at 200,000 \times magnification are



presented in Figs. 5a and b respectively. Figure 5a shows uniform distribution of nanoparticles having irregular shapes and different sizes ranging from 50 to 100 nm with a slight tendency to agglomerate. The micrograph for ZNA-3 (Fig. 5b) also illustrates irregular morphology however, the particles appear to be larger in size as compared to ZNA-1 due to the particle growth at higher calcination temperatures [35].

In fact, increase in calcination temperature results in a rapid growth in nucleation rate of the particles owing to the super-saturation of products making crystal core in a very short period of time causing nuclear aggregation with the continuous rise in temperature. Parra et al. observed increase in crystallite size from 28 to 44 nm with the rise in calcination temperature from 200 to 500 $^{\circ}\text{C}$ [36]. The agglomeration among nanoparticles also occurs due to their tendency to lower the high surface energy during their growth [37]. Actually the extent of particle aggregation is the key factor that affects the surface morphology and structure of the final product. Comparison of morphology of zinc oxide nanoparticles prepared by different routes is given in Table 1.

Table 1 Comparison of morphology of zinc oxide nanoparticles prepared by different routes

Synthesis method	Shape	Size	References
Wet chemical synthesis	Horizontal/Agglomerated	52.24 nm	Jayachandran et al. [33]
Microwave-assisted	Nanoflakes/Nanoplates	60–200 nm	Yalcin et al. [38]
Green synthesis	Hexagonal	40–45 nm	Alamdari et al. [39]
Co-precipitation	Spherical/Aggregated	80 nm	Mahmood et al. [40]
Precipitation	Spherical	20–40 nm	Ghorbani et al. [41]

Conclusion

Present study leads to the conclusion that zinc oxide nanoparticles have been synthesized successfully through sol–gel process using aqueous isopropanol as solvent and glycerin as a low-cost, non-toxic and eco-friendly polyol. A distinct combination of polyol mediated procedure and calcination induced process effectively controlled agglomeration leading to the formation of nanoparticles of different sizes between 50 and 100 nm. However, the particles combined to form agglomerates of 200–400 nm size obtained with the rise in calcination temperature from 500 to 900 °C. X-ray diffraction analysis confirmed the formation of hexagonal wurtzite structure of zinc oxide. Hence, the study reveals a simple process for the synthesis of zinc oxide nanoparticles.

Acknowledgements

Not applicable.

Author contributions

Conceptualization: SZ; investigation: SQ; resources: HB; data curation: AS; Writing: SZ; project administration: AA. The authors read and approved the final manuscript.

Funding

Not applicable.

Availability of data and materials

All data generated or analyzed during this study are included in the manuscript.

Declarations

Ethics approval and consent to participate

Not applicable.

Consent for publication

Not applicable.

Competing interests

The authors declare that they have no competing interests.

Author details

¹Mineral Processing Research Centre, PCSIR Laboratories Complex, Ferozpur Road, Lahore 54600, Pakistan. ²Department of Chemistry, Post Graduate Islamia College, Cooper Road, Lahore 54000, Pakistan. ³Food and Biotechnology Research Centre, PCSIR Laboratories Complex, Ferozpur Road, Lahore 54600, Pakistan.

Received: 23 May 2022 Accepted: 9 November 2022

Published online: 24 November 2022

References

- Geetha MS, Nagabhushana H, Shivananjaiah HN. Green mediated synthesis and characterization of ZnO nanoparticles using *Euphorbia Jatropha* latex as reducing agent. *J Sci Adv Mater Dev.* 2016;1:301–10.
- Alwan RM, Kadhim QA, Sahan KM, Ali RA, Mahdi RJ, Kassim NA, Jassim AN. Synthesis of zinc oxide nanoparticles via sol–gel route and their characterization. *Nanosci Nanotechnol.* 2015;5:1–6.
- Hasnidawani JN, Azlina HN, Norita H, Bonnia NN, Ratim S, Ali ES. Synthesis of ZnO nanostructures using sol-gel method. *Procedia Chem.* 2016;19:211–6.
- Gunalan S, Sivaraj R, Rajendran V. Green synthesized ZnO nanoparticles against bacterial and fungal pathogens. *Prog Nat Sci.* 2012;22(6):693–700.
- Balogun SW, James OO, Sanusi YK, Olayinka OH. Green synthesis and characterization of zinc oxide nanoparticles using bashful (*Mimosa pudica*), leaf extract: a precursor for organic electronics applications. *SN Appl Sci.* 2020;2:504–11.
- Yahya N, Zahari SMSNS, Ramli A, Mohamad NM, Puspitasari P, Zul NLC. Synthesis and characterization of zinc oxide nanoparticles prepared via precipitation and self-combustion methods. *AIP Conf Proc.* 2009;1136:401–5.
- Acosta-Humánez M, Montes-Vides L, Almanza-Montero O. Sol-gel synthesis of zinc oxide nanoparticle at three different temperatures and its characterization via XRD IR EPR. *DYNA.* 2016;83(195):224–8.
- Khan MF, Ansari AH, Hameedullah M, Ahmad E, Husain FM, Zia Q, Baig U, Zaheer MR, Alam MM, Khan AM, AlOthman ZA, Ahmad I, Ashraf GM, Aliev G. Sol-gel synthesis of thorn-like ZnO nanoparticles endorsing mechanical stirring effect and their antimicrobial activities: Potential role as nano-antibiotics. *Sci Rep.* 2016;6:1–12.
- Rochman NT, Akwalia PR. Fabrication and characterization of zinc oxide (ZnO) nanoparticle by sol-gel method. *J Phys Conf Ser.* 2017;853:1–5.
- Vishwakarma A, Singh SP. Synthesis of zinc oxide nanoparticle by sol-gel method and study its characterization. *Int J Res Appl Sci Eng Technol.* 2020;8(4):1625–7.
- Somoghi R, Purcar V, Alexandrescu E, Gifu IC, Ninciuleanu CM, Cotrut CM, Oancea F, Stroescu H. Synthesis of zinc oxide nanomaterials via sol-gel process with anti-corrosive effect for Cu Al and Zn metallic substrates. *Coatings.* 2021;11:444–58.
- Anzlovar A, Orel ZC, Kogej K, Zigon M. Polyol-mediated synthesis of zinc oxide nanorods and nanocomposites with poly(methyl methacrylate). *J Nanomater.* 2012;2012:1–9.
- Chen S, Zhou B, Weili Hu, Zhang W, Yin N, Wang H. Polyol mediated synthesis of ZnO nanoparticles templated by bacterial cellulose. *Carbohydr Polym.* 2013;92:1953–9.
- Wang M, Li AD, Kong JZ, Gong YP, Zhao C, Tang YF, Wu D. Fabrication and characterization of ZnO nano-clips by the polyol-mediated process. *Nanoscale Res Lett.* 2018;13:47–54.
- Mahamuni PP, Patil PM, Dhanavade MJ, Badiger MV, Shadija PG, Lokhande AC, Bohara RA. Synthesis and characterization of zinc oxide nanoparticles by using polyol chemistry for their antimicrobial and antibiofilm activity. *Biochem Biophys Rep.* 2019;17:71–80.
- Biron DS, Santos V, Bergmann CP. Synthesis and characterization of zinc oxide obtained by combining zinc nitrate with sodium hydroxide in polyol medium. *Mater Res.* 2020;23(2):e20200080–5.
- Zakiyah A, Anindika GR, Kusumawati Y. Synthesis of zinc oxide (ZnO) nanoparticles by polyol method and its application on photocatalytic reduction of paracetamol concentration. *AIP Conf Proc.* 2021;2349:020053-1–020053-7.

18. Banerjee P, Chakrabarti S, Maitra S, Dutta BK. Zinc oxide nano-particles—Sonochemical synthesis, characterization and application for photo-remediation of heavy metal. *Ultrason Sonochem.* 2012;19:85–93.
19. Wang Z, Li H, Tang F, Ma J, Zhou X. A facile approach for the preparation of nano-size zinc oxide in water/glycerol with extremely concentrated zinc sources. *Nanoscale Res Lett.* 2018;13:202–10.
20. Fereshteh Z, Loghman-Estarki MR, Razavi RS, Taheran M, Razavi RS, Loghman-Estarki MR, Farhadi-Khouzani M, Barekat M, Jamali H. Large scale synthesis of zinc oxide nano- and submicro-structures by Pechinis method: effect of ethylene glycol/citric acid mole ratio on structural and optical properties. *Curr Nanosci.* 2011;7:807–12.
21. Farhadi-Khouzani M, Fereshteh Z, Loghman-Estarki MR, Razavi RS. Different morphologies of ZnO nanostructures via polymeric complex sol–gel method: synthesis and characterization. *J Sol-Gel Sci Technol.* 2012;64:193–9.
22. Mohan AC, Renjanadevi B. Preparation of zinc oxide nanoparticles and its characterization using scanning electron microscopy (SEM) and X-ray diffraction (XRD). *Proc Technol.* 2016;24:761–6.
23. Safawo T, Sandeep BV, Pola S, Tadesse A. Synthesis and characterization of zinc oxide nanoparticles using tuber extract of anchote (*Coccinia abyssinica* (Lam.) Cong.) for antimicrobial and antioxidant activity assessment. *OpenNano.* 2018;3:56–63.
24. Kayani ZN, Saleemi F. Effect of calcination temperature on the properties of ZnO nanoparticles. *Appl Phys A.* 2015;119:1–8.
25. Lefu M, Kaiming L. Crystallization behavior of Mg-doped titania. *Key Eng Mater.* 2010;434–435:847–9.
26. Sceanovic M, Abramovic B, Golubovic A, Kler S, Grujic-Brojcin M, Dohcevic-Mitrovic Z, Babić B, Matović B, Popovic ZV. Photocatalytic degradation of metoprolol in water suspension of TiO₂ nanopowders prepared using sol–gel route. *J Sol–Gel Sci Technol.* 2012;61:390–402.
27. Sharma G, Soni R, Jasuja ND. Phytoassisted synthesis of magnesium oxide nanoparticles with *Swertia chirayaita*. *J Taibah Univ Sci.* 2017;11(3):471–7.
28. Wong M, Chen C, Hsieh C, Hung S, Sun D, Chang H. Antibacterial property of Ag nanoparticle-impregnated N-doped Titania films under visible light. *Sci Rep.* 2015;5:1–11.
29. Ramimoghdam D, Bagheri S, Hamid SBA. Biotemplated synthesis of anatase titanium dioxide nanoparticles via lignocellulosic waste material. *BioMed Res Int.* 2014;2014:1–7.
30. Meshesha DS, Matangi RC, Tirukkovalluri SR, Bojja S. Synthesis and characterization of Ba²⁺ and Zr⁴⁺ co-doped titania nanomaterial which in turn used as an efficient photocatalyst for the degradation of rhodamine-B in visible light. *S Afr J Chem Eng.* 2017;23:10–6.
31. Zahra S, Mazhar S, Zahra S, Idrees H, Hussnain A. Synthesis and characterization of magnesium doped titania for photocatalytic degradation of methyl red. *Rev Mater.* 2022;27(1):1–14.
32. Fereshteh Z, Loghman-Estarki MR, Razavi RS, Taheran M. Template synthesis of zinc oxide nanoparticles entrapped in the zeolite Y matrix and applying them for thermal control paint. *Mater Sci Semicond Process.* 2013;16:547–53.
33. Jayachandran A, Aswathy TR, Achuthsankar S. Green synthesis and characterization of zinc oxide nanoparticles using *Cayratia pedata* leaf extract. *Biochem Biophys Rep.* 2021;26:1–8.
34. Arshad M, Qayyum A, Abbas G, Haider R, Iqbal M, Nazir A. Influence of different solvents on portrayal and photocatalytic activity of tin-doped zinc oxide. *J Mol Liq.* 2018;260:1–8.
35. Zahra S, Qaisar S, Sheikh A, Bukhari H, Amin A. Effect of calcination temperature on the structure and morphology of zinc oxide nanoparticles synthesized by base-catalyzed aqueous sol-gel process. *Eur J Chem.* 2022;13(2):162–7.
36. Parra MR, Haque FZ. Aqueous chemical route synthesis and the effect of calcination temperature on the structural and optical properties of ZnO nanoparticles. *J Mater Res Technol.* 2014;3(4):363–9.
37. Srivastava N, Srivastava PC. Realizing NiO nanocrystals from a simple chemical method. *B Mater Sci.* 2010;33(6):653–6.
38. Yalcin M. Microwave-assisted synthesis of ZnO nanoflakes: structural, optical and dielectric characterization. *Mater Res Express.* 2020;7:1–11.
39. Alamdari S, Ghamsari MS, Lee C, Han W, Park H, Tafreshi MJ, Afarideh H, Ara MHM. Preparation and characterization of zinc oxide nanoparticles using leaf extract of *Sambucus ebulus*. *Appl Sci.* 2020;10:1–19.
40. Mahmood NB, Saeed FR, Gbashi KR, Mahmood U. Synthesis and characterization of zinc oxide nanoparticles via oxalate co-precipitation method. *Mater Lett: X.* 2022;13:100126–9.
41. Ghorbani HR, Mehr FP, Pazoki H, Rahmani BM. Synthesis of ZnO nanoparticles by precipitation method. *Orient J Chem.* 2015;31:1219–21.

Publisher's Note

Springer Nature remains neutral with regard to jurisdictional claims in published maps and institutional affiliations.

Ready to submit your research? Choose BMC and benefit from:

- fast, convenient online submission
- thorough peer review by experienced researchers in your field
- rapid publication on acceptance
- support for research data, including large and complex data types
- gold Open Access which fosters wider collaboration and increased citations
- maximum visibility for your research: over 100M website views per year

At BMC, research is always in progress.

Learn more biomedcentral.com/submissions

